Appl Microbiol Biotechnol (2015) 99:7757–7769
DOI 10.1007/s00253-015-6669-z

ENVIRONMENTAL BIOTECHNOLOGY

# Acetoclastic methanogenesis is likely the dominant biochemical pathway of palmitate degradation in the presence of sulfate

**Lei Lv[1] · Serge Maurice Mbadinga[1,3] · Li-Ying Wang[1] · Jin-Feng Liu[1] · Ji-Dong Gu[2] · Bo-Zhong Mu[1,3] · Shi-Zhong Yang[1]**

Received: 24 March 2015 / Revised: 29 April 2015 / Accepted: 1 May 2015 / Published online: 20 May 2015


**Abstract** Long chain fatty acids (LCFAs) are important intermediates in the anaerobic degradation of *n*-alkanes. In order to find out the biochemical processes involved in the degradation of LCFAs, palmitate (a typical LCFA) was used as a substrate, and low-temperature oilfield production fluids were used as a source of microorganisms to establish two anaerobic systems, one with addition of sulfate as exogenous electron acceptor (SP), another without exogenous electron acceptor (MP) and both incubated at room temperature. After more than 2 years of incubation, about 48 and 57.4 % of the palmitate were degraded in samples of MP and SP, respectively. Methane production reached 1408 and 1064 μmol for MP and SP, respectively. Clone libraries of archaeal 16S rRNA genes showed that the predominant archaea in the sulfate-amended cultures (SP) was *Methanosaeta* whereas *Methanocalculus* dominated the culture without addition of exogenous sulfate (MP). This observation shows that palmitate could be biodegraded into methane through β-oxidation and acetoclastic methanogenesis in the presence of with or without sulfate. The high occurrence of *Methanosaeta* in the sulfate-amended system indicates that acetoclastic methanogenesis was not inhibited/little affected by the addition of sulfate. Acetoclastic methanogenesis might be the predominant biochemchimcal pathway of methane generation in enrichment cultures amended with sulfate. These results shed light on alternative methanogenic pathways in the presence of sulfate.

**Keywords** Anaerobic degradation · Hydrogenotrophic · Acetoclastic · Methanogenesis · Palmitate · Sulfate reduction

## Introduction

Long chain fatty acids (LCFAs) are commonly found in several types of environments including wastewaters, coal mines, and petroleum reservoirs (Sousa et al. 2009; Beckmann et al. 2011). They are important intermediates in the anaerobic alkane degradation (Cravo-Laureau et al. 2005; Callaghan et al. 2006) and can form a substantial amount of the dry weigth of biomass (Sousa et al. 2009). LCFAs could be anaerobically biodegraded to generate terminal products, including methane, $CO_2$, and hydrogen gas ($H_2$) under a "conventional" β-oxidation and methanogenic conditions (Sousa et al. 2009). Thus, large amounts of biogas can be yielded via the above-mentioned biochemical processes. Biodegradation of LCFAs involves complex microbial partnerships, i.e., syntrophic communities (acetogens and methanogens) and sulfate-reducing ones.

Under methanogenic conditions, LCFAs can be degraded by syntrophic communities of acetogenic bacteria and methanogenic (hydrogenotrophic and acetoclastic) archaea to methane ($CH_4$). In wastewater systems containing abundant sulfate, previous studies indicated that methanogenesis was totally or partially inhibited since sulfate-reducing bacteria

**Electronic supplementary material** The online version of this article (doi:10.1007/s00253-015-6669-z) contains supplementary material, which is available to authorized users.

✉ Shi-Zhong Yang
meor@ecust.edu.cn

[1] State Key Laboratory of Bioreactor Engineering and Institute of Applied Chemistry, East China University of Science and Technology, Shanghai 200237, People's Republic of China

[2] School of Biological Sciences, The University of Hong Kong, Pokfulam Road, Hong Kong, SAR, People's Republic of China

[3] Shanghai Collaborative Innovation Center for Biomanufacturing Technology, Shanghai 200237, People's Republic of China

outcompeted syntrophic acetogens for fatty acids and methanogens for acetate and/or hydrogen gas ($H_2$) available (Colleran et al. 1995; Sousa et al. 2009). Oil reservoirs, inhabited by a wide array of anaerobic microorganisms, also contain many kinds of inorganic ions (sulfate, nitrate) and organic compounds (alkanes). LCFAs, such as stearate and palmitate, have also been detected in the acid fraction of crude oils, and their presence was found to be correlated with biodegradation processes (Meredith et al. 2000; Grabowski et al. 2005). However, how oil reservoir microorganisms will respond to LCFAs is still not clear. So far, biodegradation of LCFAs to methane under methanogenic conditions has been well studied, and biodegradation of LCFAs to methane in the presence of sulfate is rarely documented, and under such conditions, the competition between sulfate-reducing bacteria and methanogens is still not clear. Therefore, more studies related to LCFA degradation biochemical pathways and functional microbial communities are needed.

In the present work, palmitate, a typical LCFA as well as an important intermediate during the process of anaerobic alkane degradation (Fig. 1), was used as a substrate and oil reservoir production water as inoculum to enrich palmitate-based consortia under two different culturing conditions (with and without sulfate amendment) in order to investigate the microbial communities and the dominant biochemical processes involved. Methane formation regardless of the presence of sulfate or not shows that methanogenesis was the predominant metabolic pathway under both treatment conditions. Microbial communities were characterized by means of 16S rRNA gene cloning, and qPCR was used for group-specific quantification of acetoclastic and $CO_2$-reducing methanogens.

## Materials and methods

### Sample collection

Production water samples were collected from a crude-oil-producing well in an oil field of China. Five liters of production water sample was collected directly from the production valve of the pipeline at the well-head into sterile bottles after flushing for a minimum of 10 min. The bottles were completely filled with oil/water mixture, tightly sealed, and immediately transported back to laboratory for treatment.

### Enrichment and culturing

Initial culture was established by transferring 80 ml of production water into a 120-ml sterilized serum bottle containing 0.1 mg/l of resazurin. Before capped with butyl rubber stoppers, the bottles were flushed with pure $N_2$ (99.99 %), after passing through heated copper filings to remove trace of oxygen for 10 min. After about 3 months of incubation at room temperature (22±1 °C), the microcosm was then flushed with pure $N_2$ to remove $CH_4$ and $CO_2$. Enrichment cultures were then established by transferring 5 ml of the initial culture content described above into each fresh 120-ml serum bottle containing 50 ml of anaerobic basal medium. The basal medium contained the following (g/l): NaCl, 1.0; $MgCl_2 \cdot 6H_2O$, 0.4; $CaCl_2 \cdot 2H_2O$, 0.075; $NH_4Cl$, 0.25; $KH_2PO_4$, 0.75; $K_2HPO_4$, 1.16; KCl, 0.5; and resazurin, 0.0001. For establishment of sulfate-reducing conditions, 4.0 g/l of $Na_2SO_4$ was added to the above basal medium. The medium was further supplemented with 1.0 ml of trace elements and 1.0 ml of vitamin stock solution. The trace elements and vitamin stock solutions were prepared according to those described by Wang et al. (2011). Palmitate (10 mM) was added as the carbon and energy sources to these microcosms. All microcosms were prepared in triplicate. Treatments used herein were denoted as follows: M0 (control without palmitate or sulfate addition), MP (amended with palmitate only), S0 (control without palmitate but with sulfate addition), SP (incubation amended with both palmitate and sulfate).

### Headspace gas and acid metabolite analysis

Headspace gas was measured by injecting 200 μl from culturing serum bottle onto a gas chromatograph equipped with a flame ionization detector (FID), a thermal conductivity detector (TCD). and a packed 1.5-m stainless steel column filled with 5 Å carbon molecular sieves. Both the injector and the detectors were held at 200 °C. The column temperature was initially held at 60 °C for 12 min, increased at a rate of 15 °C/min to 200 °C and kept at this final temperature for 24 min. $N_2$ was used as the carrier gas, and the flowing rate was 22.3 ml/min. Analysis of acidic metabolites was carried out at the end of the incubation period. Both volatile fatty acids (VFAs) and LCFAs were measured at the end of the incubation according to the methods described previously (Mbadinga et al. 2012; Zhou et al. 2012).

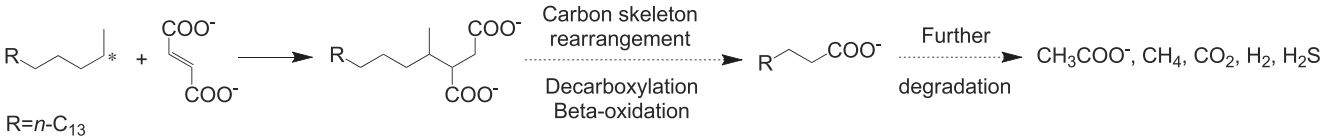


**Fig. 1** Biochemical strategy for the anaerobic formation of palmitate, as intermediate, from the metabolism of octadecane with fumarate addition as the initial activation: by addition of fumarate, substrate carbon skeleton rearrangement, and decarboxylation, an intermediate, palmitate is produced, which is furtherly converted to methane and other metabolites

### DNA extraction and PCR amplification

Genomic DNA was extracted from 13 ml of enrichment culture using AxyPrep™ bacterial Genomic DNA Miniprep Kit (Axygen Biosciences, Inc., CA, USA) according to the manufacturer's protocol. Extracted genomic DNAs were immediately frozen and stored at −70 °C for further use. Partial 16S rRNA genes were amplified using the primers 8F (5′-AGAG TTTGATYMTGGCTCAG-3′) and 805R (5′-GACTACCA GGGTATCTAATCC-3′) for bacteria (Savage et al. 2010; Mbadinga et al. 2012; Zhou et al. 2012); primers ARC109F (5′-ACKGCTCAGTAACACGT-3′) and ARC915R (5′-GTGCTCCCCCGCCAATTCCT-3′) for archaea (Cheng et al. 2007; Zhou et al. 2012). The thermal program for primers 8F/805R and ARC109F/ARC915R was carried out according to the description of Zhou et al. (2012).

All PCR products obtained above were first visualized on agarose gel (1 %, *w*/*v*) electrophoresis followed by gel staining (DuRed nucleic acid gel stain, Beijing, China) to ensure that the correct size fragment was amplified. Subsequently, PCR products resulted from two independent reactions (each containing 50 μl of PCR reaction mixture) were pooled and visualized on agarose gel (1.8 %, *w*/*v*) electrophoresis (50 min at 160 V). The appropriately sized fragments were excised and purified with a DNA purification kit (Axygen® Biosciences, Inc., CA, USA) prior to cloning.

### Construction of 16S rRNA gene clone libraries

Purified 16S rRNA gene fragments were directly cloned into *Escherichia coli* using pMD19®-T Simple cloning vector (Takara, Japan) following the instructions of the manufacturer. Obtained white colonies were picked randomly and cultured overnight at 37°C in 0.8 ml of LB medium in the presence of ampicillin (50 mg/l). The insertion of 16S rRNA gene was checked by PCR using M13F (-47)/RV-M plasmid specific primers (Guan et al. 2013), followed by agarose gel electrophoresis and staining with DuRed nucleic acid gel stain. Obtained sequences were checked for vector contamination by VecScreen software (www.ncbi.nlm.nih.gov/tools/vecscreen/) before further use.

### PCR amplification of archaeal 16S rRNA genes and DGGE analysis

Archaea oligonucleotides A109F (ACKGCTCAGTAACAC GT) and GC-A515R (CGCCCGCCGCGCGCGGCGGGCG GGCGGGGGCACGGGGGGTTACCGCGGCGGCTGGC A) were used for amplification of universal archaeal 16S rRNA genes. PCR amplification of samples was prepared according to the description of Guan et al. (2014). PCR reaction was performed as follows: 5 min for initial denaturation of DNA at 94 °C, followed by 42 cycles of 45-s denaturation at 94 °C, 1-min primer annealing at 52 °C and 1-min extension at 72 °C. Amplification was completed by a final extension step at 72 °C for 10 min. DGGE was performed using the Bio-Rad D gene system (Bio-Rad, Hercules, CA) according to the protocol of Guan et al. (2014). PCR fragments were loaded onto 6 % (*w*/*v*) polyacrylamide gels in 1× TAE (20 mM Tris, 10 mM acetate, 0.5 mM EDTA, pH 7.4). To separate the amplified DNA fragments, the polyacrylamide gels were made with denaturing gradients ranging from 30 to 60 %. The electrophoresis was run at 60 °C and 160 V for 4.5 h. Randomly selected bands of interest were isolated from the gel using a sterile tip, and the DNA containing acryl amide fragments were incubated in sterile PCR water for about 10 h to allow DNA diffusion into the sterile water. The solution was directly used for further amplifications using primer set A109F-GC-M13R (CAGGAAACAGCTATGACGGGCG GGGCGGGGGCACGGGGGGACKGCTCAGTAACAC GT)/A515R-GC-M13R(GTAAAACGACGGCCAGTAAA TAAAATAAAAATGTAAAAAATTACCGCGGCGGCT GGCA, and PCR reactions were performed with the above mentioned. Obtained PCR products were determined with automated ABI 3730 sequencer (Dye-Terminator Cycle Sequencing; Applied Biosystems), and the obtained sequences were also checked for vector contamination by VecScreen software (www.ncbi.nlm.nih.gov/tools/vecscreen/) before further use.

### Phylogenic analysis

16S rRNA gene sequences from each respective library were checked with Bellerophon (Huber et al. 2004) and Pintail (Ashelford et al. 2006) to remove chimeric sequences. Sequences with more than 97 % similarity were assembled into the same operational taxonomic units (OTUs) using CD-HIT (Fu et al. 2012; Li and Godzik 2006). From each OTU, one representative sequence was chosen to compare with sequences in the BLAST network service at http://www.ncbi.nlm.nih.gov/blast/ (Altschul et al. 1990; McGinnis and Madden 2004).

### Quantitative PCR analysis

Three pairs of PCR primers were used to detect Archaea (ARC787F/ARC1059R), *Methanomicrobiales* (MMB282F/832R), and *Methanosaicinales* (MSL812/MSL1159R) according to Yu et al. (2005). All qPCR reactions were performed using 20-μl reaction mix with 10 μl of Universal SYBR Green Master Mix, 4 μl of $ddH_2O$, 0.5 μl of forward primer, 0.5 μl of reverse primer, and 2-μl template DNA (56.7 ng/μl for MP and 44.3 ng/μl for SP). A control without the corresponding template DNA was included in every qPCR assay for each primer sets. All experiments were conducted in triplicate. For ARC and MMB sets, qPCR were performed as

follows: an initial 5-min incubation at 95 °C; 45 cycles of denaturation at 94 °C for 45 s; annealing at 63 °C for 45 s; and extension at 72 °C for 45 s. For MSL, sets were as follows: an initial 5-min incubation at 95 °C; 50 cycles of denaturation at 94 °C for 20 s; annealing at 62 °C for 30 s, and extension at 72 °C for 45 s. Results obtained from qPCR were converted into cell number by dividing 16S rRNA gene abundances (copies/ml) by the rRNA gene copy number for the different methanogens analyzed (Gray et al. 2011). The copy numbers were obtained from the ribosomal RNA operon copy number database at https://rrndb.umms.med.umich.edu/ (*Methanomicrobiales* 1–4 copies, *Methanosarcinales* 1–3 copies) (Lee et al. 2009).

### Nucleotide sequence accession numbers

Partial 16S rRNA gene sequences of bacteria and archaea obtained in this study were deposited in the GenBank database under accession numbers: KJ468589-KJ468597 for M0-A, KJ468477-KJ468495 for M0-B, KJ468525-KJ468534 for S0-A, KJ468535-KJ468565 for S0-B, KJ468598-KJ468611 for MP-A, KJ468496-KJ468513 for MP-B, KJ468514-KJ468524 for SP-A, and KJ 468566-KJ468588 for SP-B (A and B for archaea and bacteria, respectively).

### Thermodynamic calculations

Gibbs free energy data for palmitate were taken from Noor et al. (2013). For all other compounds, the data information and Gibbs free energy calculations were made according to Thauer et al. (1977) and Amend and Shock (2001). Table 2 lists the changes in Gibbs free energy values for various reactions for anaerobic LCFA degradation. The change in Gibbs free energy ($\Delta G°$) for the conversion of palmitate to hydrogen and carbon dioxide according to reaction [1] $C_{16}H_{31}O_2^- + 30H_2O + H^+ = 16CO_2 + 46H_2$ is 1104.87 kJ/mol palmitate (Thauer et al. 1977; Noor et al. 2013). Hence, at pH=7 $\Delta G' = 1104.9 - RT\ln([C_{16}H_{31}O_2^-]/[CO_2]^{16}[H_2]^{46})$ (in biological systems $\ln[H_2O]$ is assumed to be 0, Dolfing et al. (2008)). Therefore, under otherwise standard conditions, $\Delta G' = 1104.9 + 262.66 \log[H_2]$ (where $5.71\log x$ equals $RT_{298.15}\ln x$; $5.71 \log[H_2]^{46} = 262.66 \log[H_2]$). As the threshold value is the value where $\Delta G' = 0$, it follows that $[H_2] = 10^{(-1104.87/262.66)} = 10^{-4.21}$. Thus, $[H_2]_{crit} = 6.2 \times 10^{-5}$ atm. Similarly, the $[H_2]_{crit}$ and $[CH_3COO^-]_{crit}$ of reaction [2] $4H_2 + CO_2 = CH_4 + 2H_2O$ and reaction [3] $CH_3COO^- + H^+ = CH_4 + CO_2$ were $1.89 \times 10^{-6}$ atm and $5.4 \times 10^{-7}$ M, respectively, according to Jan Dolfing et al. (2008, 2009, 2014). The change in Gibbs free energy ($\Delta G°$) for the conversion of palmitate to hydrogen and carbon dioxide according to reaction [4] $C_{16}H_{31}O_2^- + 14H_2O = 8CH_3COO^- + 14H_2 + 7H^+$ is 345 kJ/mol palmitate. Hence, at pH=7 $\Delta G' = 345 - RT\ln([C_{16}H_{31}O_2^-]/[CH_3OO^-]^8[H_2]^{14})$. Therefore, under otherwise standard conditions, $\Delta G' = 345 + 5.71 \log[CH_3COO^-]^8 [H_2]^{14}$. As the threshold value is the value where $\Delta G' = 0$, it follows that $\log[CH_3COO^-] = -7.55 - 1.75\log[H_2]$, with $H_2$ in atm and $[CH_3COO^-]$ in M. In this work, other reactions were similarly calculated as described above.

## Results

### Physicochemical characteristics of the production water

The production water samples were obtained from a depth of 480 m below ground, with in situ temperature and pressure estimated at 21 °C and 7.58 MPa, respectively. The production water contained approximately 3.21 g/l of $Cl^-$, 2.88 g/l of $\sum(Na^+ + K^+)$, 0.078 g/l of $Ca^{2+}$, 0.035 g/l of $Mg^{2+}$, $SO_4^{2-}$ and $HCO_3^-$ were 0.07 and 2.46 g/l. Acetate was approximately 29.8 mg/l (0.5 mM), and other VFAs were not detectable.

### $CH_4$ production and metabolite formation in incubation

**MP incubation** The oil reservoir production water amended with palmitate was incubated under anaerobic conditions. Headspace methane was monitored in all the microcosms at frequent time intervals during the incubation period (770 days). An increase in the amount of methane production was observed, and methane was accumulated in the headspace of the serum bottles reaching 1323 μmol/microcosm above the controls (M0) on day 770 (Fig. 2). In the control (M0)

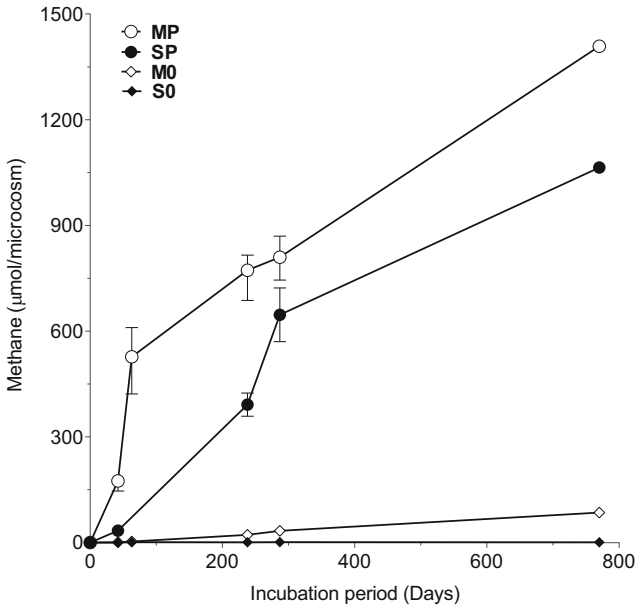


**Fig. 2** Methane production during the incubation period (770 days). A total of 1408, 1064, 85.26, and 0.77 μmol $CH_4$ were produced, respectively, from MP, SP, M0, and S0

incubations, methane was generated to a much less extent, reaching 85.26 μmol/microcosm on day 770, therefore indicating that a large portion of the methane generated derived from the degradation and conversion of palmitate. This information also suggests that the oil reservoir production water harbors microbial community capable for the degradation and conversion of palmitate to methane. At the end of the incubation, 259.73 palmitate was detected, indicating that 240.27 μmol/microcosm palmitate was utilized during the long-term incubation. According to reaction: [5] $palmitate^{-}+7H_2O+H^{+}=11.5CH_4+4.5CO_2$, $\Delta G^{o'}$=-398.6 kJ $mol^{-1}$ (Thauer et al. 1977; Sousa et al. 2010), and assuming that all the palmitate utilized was converted into methane, 2763.1 μmol methane/microcosm will be theoretically produced. Our data indicate that 1408 μmol methane/microcosm for MP, accounting for 51.0 % of the theoretical value. At the same time, $H_2$ and $CO_2$ were also analyzed during the incubation; VFAs such as formate, acetate, propionate, and butyrate were detected, and the results are shown in Table 1.

**SP incubation** Headspace methane was also monitored in all the microcosms at frequent time intervals during the incubation period (770 days). Substantial amounts of methane were accumulated in the headspace of the serum bottles, reaching 1063 μmol/microcosm above the controls (S0) on day 770 (Fig. 2). In contrast, methane was produced to a much less extent in the controls (S0), reaching 0.52 μmol/microcosm on day 770, therefore indicating that a large portion of the methane generated derived from the degradation and conversion of palmitate, suggesting that the oil reservoir production water harbors microbial community capable of bioconversion of palmitate to methane in the presence of sulfate. At the end of the incubation, 212.93 μmol/microcosm of palmitate was detected, indicating that 287.07 μmol/microcosm palmitate was utilized during the long-term incubation. According to reaction: [6] $palmitate^{-}+3.5SO_4^{2-}+8H^{+}=8CH_4+8CO_2+3.5H_2S$, $\Delta G^{o'}$=-493.1 kJ $mol^{-1}$ (Thauer et al. 1977; Sousa et al. 2010; Rabus et al. 2013), and assuming that all the palmitate utilized in SP was converted into methane, theoretical methane yield should reach 2296.6 μmol/microcosm, indicating that 1064 μmol methane/microcosm accounted for 46.3 % of the theoretical value. At the same time, $H_2$ was not detected, $CO_2$ production reached 337.9 μmol/microcosm after incubation; VFAs such as formate, acetate, propionate, and butyrate were also analyzed (Table 1).

## Microbial community based on 16S rRNA gene of MP

At the end of the incubation period, DNA was extracted from MP and SP cultures and subjected to PCR amplification using PCR primer sets specific for bacteria and archaea, and then, 16S rRNA gene clone libraries were constructed. For MP sample, 42 and 37 clones were randomly selected for the domains of bacteria and archaea, respectively. After screening all the sequences in CD-HIT, there were 18 and 9 operational taxonomy units (OTUs) obtained from MP for bacteria and archaea, respectively. As shown in Fig. 3, about 61.9 % of the bacterial sequences obtained were affiliated with members of the phylum *Thermotogae* and MP-T6190 cluster (most were affiliated with unclassified Bacteria). Other bacterial sequences detected in MP-B were affiliated with the phyla *Bacteroidetes* (14.2 %), *Cloacimonetes* (4.8 %), *Chloroflexi* (9.5 %), *Firmicutes* (2.4 %), Candidate division JS1 (2.4 %), *Artribacteria* (2.4 %), and *Proteobacteria* (2.4 %). Phylogenetic affiliation of Bacterial 16S rRNA gene clones detected in sample M0 is shown as Table S1 in Supplementary materials. Compared with the controls M0 (Table S2), archaeal sequences obtained from MP-A were all affiliated with the phylum *Euryarchaeota* and subdivided into the orders *Methanomicrobiales* and *Methanosarcinales* (Fig. 4) among which 83.8 % of all archaeal sequences fell within the order *Methanomicrobiales* and mainly represented by $CO_2$-reducer members of the genus *Methanocalculus*. Within the order *Methanomicrobiales*, OTU represented by clone A16-7 shared 99 % identity to *Methanocalculus* (JF947120), which has been detected from a crude oil-contaminated soil (Cheng et al. 2014) and crude oil alkane degrading consortium (Gray et al. 2011). OTU represented by clone A16-4 and A16-27 shared 95 and 99 % identity to a groundwater sample isolated strain *Methanosarcina spelaei* (LC006853), respectively (Shimizu et al. 2011). Other OTUs (10.8 % of total archaeal clones) represented by A16-57, A16-11, and A16-29 are

**Table 1** Metabolites (μmol/microcosm) detected for different enrichment cultures after incubation for 770 days

| Samples | Palmitate added (μmol) | Palmitate remained (μmol) | $SO_4^{2-}$ | $CH_4$ | $CO_2$ | $H_2$ | Formate | Acetate | Propionate | Butyrate |
|---|---|---|---|---|---|---|---|---|---|---|
| M0 | - | - | 0.37 | 85.26 | 10.09 | nd | 44.73 | 18.31 | 0.4345 | 0.0605 |
| S0 | - | - | 1335 | 0.77 | 0.5183 | nd | 83.67 | 27.93 | 0.22 | 0.050 |
| MP | 500 | 259.7 | 7.54 | 1408 | 312.4 | nd | 192.5 | 110.6 | 0.0495 | nd |
| SP | 500 | 212.9 | 6.13 | 1064 | 337.9 | nd | 27.78 | 133 | 551.4 | nd |

$SO_4^{2-}$ was analyzed by ion chromatography

*nd* not detectable

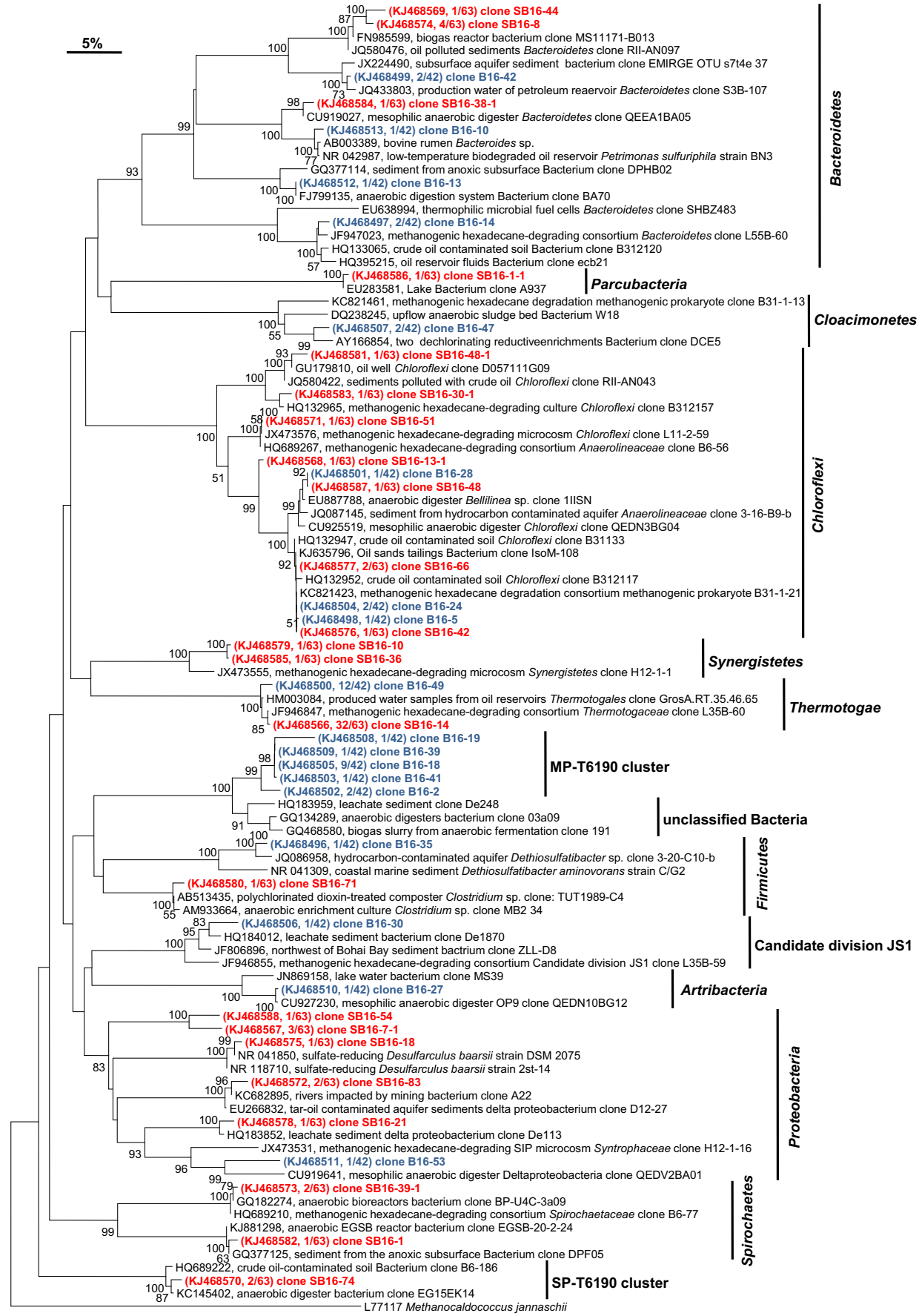
5%
(KJ468569, 1/63) clone SB16-44
(KJ468574, 4/63) clone SB16-8
FN985599, biogas reactor bacterium clone MS11171-B013
JQ580476, oil polluted sediments Bacteroidetes clone RII-AN097
JX224490, subsurface aquifer sediment bacterium clone EMIRGE OTU s7t4e 37
(KJ468499, 2/42) clone B16-42
JQ433803, production water of petroleum reaervoir Bacteroidetes clone S3B-107
(KJ468584, 1/63) clone SB16-38-1
CU919027, mesophilic anaerobic digester Bacteroidetes clone QEEA1BA05
(KJ468513, 1/42) clone B16-10
AB003389, bovine rumen Bacteroides sp.
NR 042987, low-temperature biodegraded oil reservoir Petrimonas sulfuriphila strain BN3
GQ377114, sediment from anoxic subsurface Bacterium clone DPHB02
(KJ468512, 1/42) clone B16-13
FJ799135, anaerobic digestion system Bacterium clone BA70
EU638994, thermophilic microbial fuel cells Bacteroidetes clone SHBZ483
(KJ468497, 2/42) clone B16-14
JF947023, methanogenic hexadecane-degrading consortium Bacteroidetes clone L55B-60
HQ133065, crude oil contaminated soil Bacterium clone B312120
HQ395215, oil reservoir fluids Bacterium clone ecb21
(KJ468586, 1/63) clone SB16-1-1
EU283581, Lake Bacterium clone A937
KC821461, methanogenic hexadecane degradation methanogenic prokaryote clone B31-1-13
DQ238245, upflow anaerobic sludge bed Bacterium W18
(KJ468507, 2/42) clone B16-47
AY166854, two dechlorinating reductiveenrichments Bacterium clone DCE5
(KJ468581, 1/63) clone SB16-48-1
GU179810, oil well Chloroflexi clone D057111G09
JQ580422, sediments polluted with crude oil Chloroflexi clone RII-AN043
(KJ468583, 1/63) clone SB16-30-1
HQ132965, methanogenic hexadecane-degrading culture Chloroflexi clone B312157
(KJ468571, 1/63) clone SB16-51
JX473576, methanogenic hexadecane-degrading microcosm Chloroflexi clone L11-2-59
HQ689267, methanogenic hexadecane-degrading consortium Anaerolineaceae clone B6-56
(KJ468568, 1/63) clone SB16-13-1
(KJ468501, 1/42) clone B16-28
(KJ468587, 1/63) clone SB16-48
EU887788, anaerobic digester Bellilinea sp. clone 1IISN
JQ087145, sediment from hydrocarbon contaminated aquifer Anaerolineaceae clone 3-16-B9-b
CU925519, mesophilic anaerobic digester Chloroflexi clone QEDN3BG04
HQ132947, crude oil contaminated soil Chloroflexi clone B31133
KJ635796, Oil sands tailings Bacterium clone IsoM-108
(KJ468577, 2/63) clone SB16-66
HQ132952, crude oil contaminated soil Chloroflexi clone B312117
KC821423, methanogenic hexadecane degradation consortium methanogenic prokaryote B31-1-21
(KJ468504, 2/42) clone B16-24
(KJ468498, 1/42) clone B16-5
(KJ468576, 1/63) clone SB16-42
(KJ468579, 1/63) clone SB16-10
(KJ468585, 1/63) clone SB16-36
JX473555, methanogenic hexadecane-degrading microcosm Synergistetes clone H12-1-1
(KJ468500, 12/42) clone B16-49
HM003084, produced water samples from oil reservoirs Thermotogales clone GrosA.RT.35.46.65
JF946847, methanogenic hexadecane-degrading consortium Thermotogaceae clone L35B-60
(KJ468566, 32/63) clone SB16-14
(KJ468508, 1/42) clone B16-19
(KJ468509, 1/42) clone B16-39
(KJ468505, 9/42) clone B16-18
(KJ468503, 1/42) clone B16-41
(KJ468502, 2/42) clone B16-2
HQ183959, leachate sediment clone De248
GQ134289, anaerobic digesters bacterium clone 03a09
GQ468580, biogas slurry from anaerobic fermentation clone 191
(KJ468496, 1/42) clone B16-35
JQ086958, hydrocarbon-contaminated aquifer Dethiosulfatibacter sp. clone 3-20-C10-b
NR 041309, coastal marine sediment Dethiosulfatibacter aminovorans strain C/G2
(KJ468580, 1/63) clone SB16-71
AB513435, polychlorinated dioxin-treated composter Clostridium sp. clone: TUT1989-C4
AM933664, anaerobic enrichment culture Clostridium sp. clone MB2 34
(KJ468506, 1/42) clone B16-30
HQ184012, leachate sediment bacterium clone De1870
JF806896, northwest of Bohai Bay sediment bactrium clone ZLL-D8
JF946855, methanogenic hexadecane-degrading consortium Candidate division JS1 clone L35B-59
JN869158, lake water bacterium clone MS39
(KJ468510, 1/42) clone B16-27
CU927230, mesophilic anaerobic digester OP9 clone QEDN10BG12
(KJ468588, 1/63) clone SB16-54
(KJ468567, 3/63) clone SB16-7-1
(KJ468575, 1/63) clone SB16-18
NR 041850, sulfate-reducing Desulfarculus baarsii strain DSM 2075
NR 118710, sulfate-reducing Desulfarculus baarsii strain 2st-14
(KJ468572, 2/63) clone SB16-83
KC682895, rivers impacted by mining bacterium clone A22
EU266832, tar-oil contaminated aquifer sediments delta proteobacterium clone D12-27
(KJ468578, 1/63) clone SB16-21
HQ183852, leachate sediment delta proteobacterium clone De113
JX473531, methanogenic hexadecane-degrading SIP microcosm Syntrophaceae clone H12-1-16
(KJ468511, 1/42) clone B16-53
CU919641, mesophilic anaerobic digester Deltaproteobacteria clone QEDV2BA01
(KJ468573, 2/63) clone SB16-39-1
GQ182274, anaerobic bioreactors bacterium clone BP-U4C-3a09
HQ689210, methanogenic hexadecane-degrading consortium Spirochaetaceae clone B6-77
KJ881298, anaerobic EGSB reactor bacterium clone EGSB-20-2-24
(KJ468582, 1/63) clone SB16-1
GQ377125, sediment from the anoxic subsurface Bacterium clone DPF05
HQ689222, crude oil-contaminated soil Bacterium clone B6-186
(KJ468570, 2/63) clone SB16-74
KC145402, anaerobic digester bacterium clone EG15EK14
L77117 Methanocaldococcus jannaschii
Bacteroidetes
Parcubacteria
Cloacimonetes
Chloroflexi
Synergistetes
Thermotogae
MP-T6190 cluster
unclassified Bacteria
Firmicutes
Candidate division JS1
Artribacteria
Proteobacteria
Spirochaetes
SP-T6190 cluster

◀ **Fig. 3** Phylogenetic relationships of bacterial 16S rRNA gene sequences detected in MP enrichment cultures (*in blue*) and SP enrichment cultures (*in red*). Values below 50 % are not shown. Sequences are shown with their corresponding GenBank accession number. The tree was rooted with outgroup sequence from *Methanocaldococcus jannaschii* (L77117). GenBank was accessed on between October and November 2014. *The scale bar* represents 5 % nucleotide substitution

closely related to 16S rRNA gene sequences from the genus *Methanosaeta*, which is known as a group of methanogens that use acetate as the sole energy source for growth and methanogenesis (Kendall and Boone 2006).

### Microbial community based on 16S rRNA gene of SP

For SP sample, 63 and 44 clones were selected for bacteria and archaea, and they corresponded to 23 and 8 OTUs, respectively. Bacterial OTUs retrieved from SP-B were associated with the phyla *Bacteroidetes* (9.5 %), *Parcubacteria* (1.6 %), *Chloroflexi* (12.7 %), *Synergistetes* (3.2 %), *Thermotogae* (50.8 %), *Firmicutes* (1.6 %), *Proteobacteria* (12.7 %), *Spirochaetes* (4.7 %), and other poorly characterized bacteria which are labeled SP-T6190 cluster (3.2 %) (Fig. 3). Among them, sequences affiliated with *Thermotogae* were the most encountered, representing 50.8 % of all bacterial sequences obtained from SP-B sample. The group *Proteobacteria* was mainly represented by clones affiliated with *Desulfococcus* (clones SB16-54 and SB16-7-1), *Desulfarculus* (clone SB16-18), and unclassified *Desulfobulbaceae* (clone SB16-83) as well as *Smithella* (clone clone SB16-21). Phylogenetic affiliation of bacterial 16S rRNA gene clones detected in sample S0 is shown as Table S1 in Supplementary materials. Compared with the controls S0 (Table S2), archaeal sequences obtained from SP-A were all related to 16S rRNA gene sequences of the phylum *Euryarchaeota*. Of the sequences obtained, six OTUs representing about 93.2 % of all archaeal sequences in SP-A were classified as the acetoclastic *Methanosaeta* (Fig. 4), in which 36 clones represented by SA16-28 (81.8 % of archaeal clones) showed high identity (99 %) to clone NS2-48F10 (EU722271) identified from a mesophilic petroleum reservoir production water (Pham et al. 2009) and 98 % similarities with *Methanosaeta harundinacea* $6Ac^T$ (NR102896), isolated from an UASB reactor (Zhu et al. 2012). Additional two OTUs were associated with the genus *Methanoculleus* and *Methanocalculus*, respectively. OTUs represented by SA16-33 (2.3 % of archaeal clones) showed 96 % similarities with *Methanoculleus palmolei*, a hydrogenotrophic methnaogen isolated from a biogas reactor of a palm oil plant (Zellner et al. 1998). OTUs represented by SA16-4 (4.5 % of archaeal clones) showed 99 % similarities with *Methanocalculus halotolerans*, which could utilize $H_2/CO_2$ and formate as substrates of methanogensis, was isolated from an off shore oil well (Lai et al. 2002).

### Archaeal community by DGGE

The phylogenetic affiliation of the archaeal-DGGE gene sequences is presented in Fig. S1. A total of eleven sequences were found among DGGE bands (1–11). Five bands (2, 3, 4, 5, and 6) were related with the genus *Methanosaeta*, and of the five bands three (2, 3, and 6) were affiliated with sample SP. Two bands (1 and 10) related to the genus *Methanocalculus* were affiliated with sample MP. Bands 8 and 9 related to *Methanobacterium* and *Methanosarcina*, respectively, were also detected in sample MP. The remaining two bands detected in sample M0 and sample S0 were related to *Thermoprotei* and *Methanopyri*, respectively. The results of the DGGE closely correlated with those of the analysis of the 16S rRNA gene clone libraries.

### Quantification of Archaea, *Methanomicrobiales*, and *Methanosaicinales* by quantitative PCR

The quantitative PCR of 16S rRNA genes of Archaea, *Methanomicrobiales*, and *Methanosarcinales* from two palmitate-degrading enrichment cultures was performed in BioRad CFX96 thermocycler. In the qPCR reactions, the efficiency was between 93.1 and 120 %, $R^2$ values were above 0.958 ($n$=3). The qPCR assays of the archaeal 16S rRNA genes showed that sample MP contained $2.48\times10^9$ copies/ml of archaeal while SP has $6.65\times10^8$ copies/ml. Sample MP contained $2.24\times10^9$ copies/ml ($5.60\times10^8$–$2.24\times10^9$ cells/ml) of the order *Methanomicrobiales* and $1.25\times10^9$ copies/ml ($4.17\times10^8$–$1.25\times10^9$ cells/ml) of *Methanosarcinales*; sample SP contains $6.67\times10^8$ copies/ml ($2.22\times10^8$–$6.67\times10^8$ cells/ml) of the order *Methanosarcinales* and $6.99\times10^6$ copies/ml ($1.75\times10^6$–$6.99\times10^6$ cells/ml) of *Methanomicrobiales*.

### Thermodynamics of methanogenic palmitate degradation

In this study, palmitate was chosen as an example of a typical LCFA and evaluate the thermodynamics of five possible routes of palmitate degradation (with and without the addtion of sulfate):

As shown in Table 3 (route 1), reaction [1, 7] and their sum [5] indicate that palmitate was first biodegraded to $CO_2$ and $H_2$, and then, $H_2$ and $CO_2$ were converted to methane through methanogenesis from $CO_2$ reduction.

In route 2 (Tables 2 and 3), reaction [8, 9, 10] and their sum [5] suggest that palmitate was first biodegraded to acetate and $H_2$, then acetate was converted to methane and $CO_2$ through acetoclastic methanogenesis. At the same time, $H_2$ and $CO_2$ were also converted to methane though methanogenesis from $CO_2$ reduction.

Route 3 (Table 3) shows the bioconversion of palmitate to acetate and $H_2$ (reaction [8]), indicative of syntrophic acetate oxidation (reaction [11]) and methanogenesis from $CO_2$ reduction (reaction [7]).

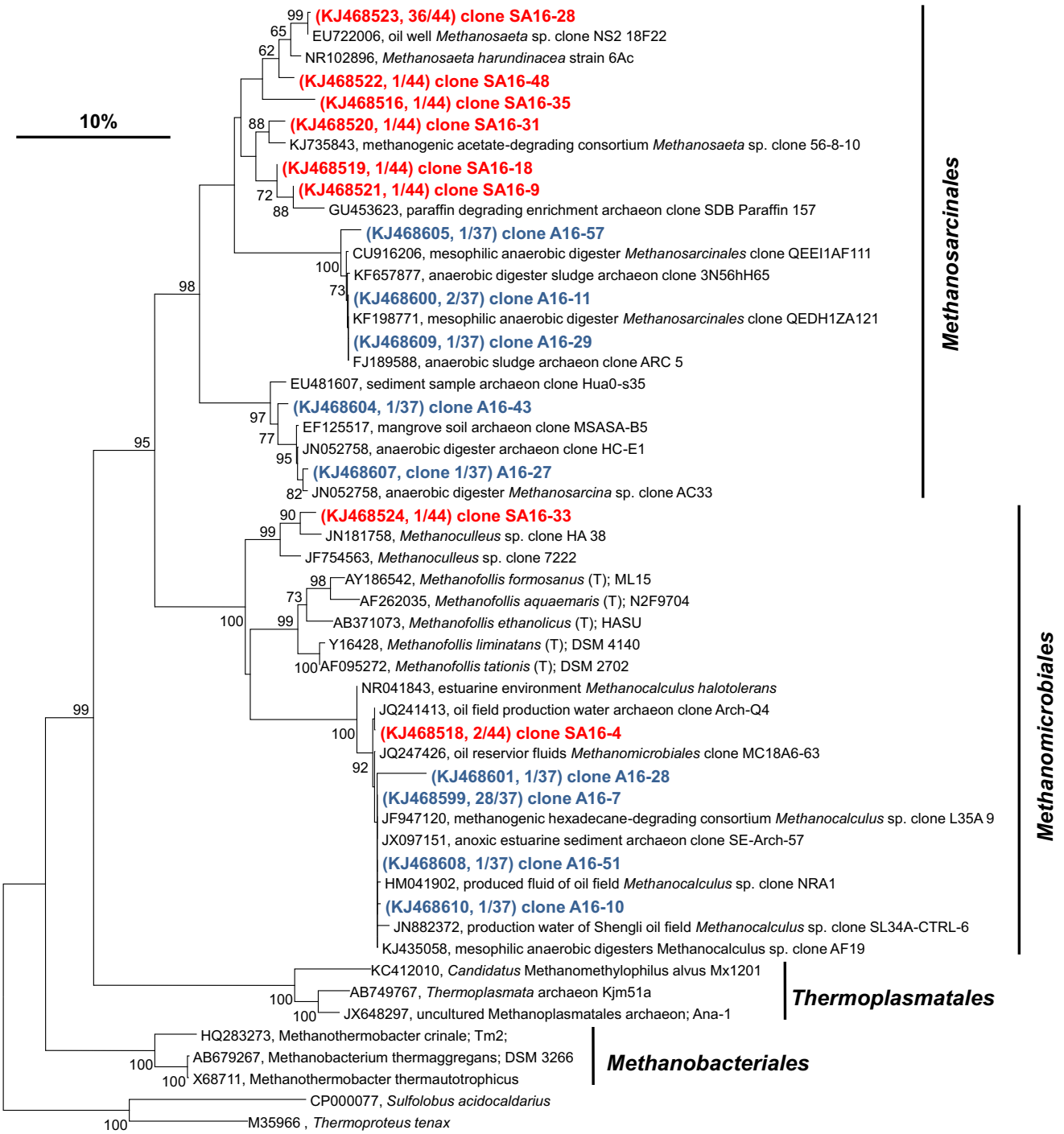


**Fig. 4** Phylogenetic relationships of archaeal 16S rRNA gene sequences detected in MP enrichment cultures (*in blue*) and SP enrichment cultures (*in red*). Values below 60 % are not shown. Sequences are shown with their corresponding GenBank accession number. The tree was rooted with outgroup sequences from *Sulfolobus acidocaldarius* (CP000077) and *Thermoproteus tenax* (M35966). GenBank was accessed between October and November 2014. The *scale bar* represents 5 % nucleotide substitution

In sulfate addition conditions (route 4, Table 3), methanogenesis of palmitate (reaction [6]) degradation mainly consists of two parts: It was biodegraded to acetate and $H_2S$ according to reaction [12], then acetate was converted to methane and $CO_2$ through acetoclastic methanogenesis according to reaction [9].

Route 5 (Table 3) also shows under sulfate amendment that palmitate was converted to acetate and $H_2S$

**Table 2** Change in Gibbs free energy ($\Delta G°$) values for the methanogenic conversion of selected LCFAs[a]

| Compound | Substrates | | Products | kJ/reaction | kJ $mol^{-1}$ | kJ $mol^{-1}$ $CH_4$ |
|---|---|---|---|---|---|---|
| Myristate | $2C_{14}H_{27}O_2^- + 12H_2O + 8H^+$ | → | $20CH_4 + 8CO_2$ | −456.2 | −228.1 | −22.8 |
| Palmitate | $2C_{16}H_{31}O_2^- + 14H_2O + 2H^+$ | → | $23CH_4 + 9CO_2$ | −797.2 | −398.6 | −34.7 |
| Stearate | $2C_{18}H_{35}O_2^- + 16H_2O + 2H^+$ | → | $26CH_4 + 10CO_2$ | −895.9 | −448.0 | −34.5 |

[a] Data for standard conditions (25 °C, solutes at 1 M concentrations, and gases at a partial pressure of 1 atm)

first. However, syntrophic acetate oxidation (reaction [11]) and methanogenesis from $CO_2$ reduction (reaction [13]) contributed to the methane production in the following steps.

In sample MP, since no sulfate was added, methanogenesis of palmitate might take place according to routes 1, 2, and 3. Palmitate could be completely/partially converted to $CO_2/H_2$ and acetate, which are all methanogenic precursors. Routes 4 and 5 were the possible methanogenic reactions of sample SP, in which sulfate reducers might contribute more to acetate production. All the above routes are summarized in Fig. 5.

## Discussion

This study examined the microbial communities of two microcosms cultured with/without sulfate as electron acceptor, and methane production was analyzed during the culturing, which illustrates the possibility that the addition of electron acceptor can alter the in situ methanogenic pathway and led to the dominance of different methanogens.

### Methane formation in MP

Anaerobic degradation of palmitate to methane requires the mutual dependence of different types of microorganisms (Sousa et al. 2007). In MP enrichment, methane production reached 1408 μmol/microcosm at the end of the incubation (770 days), which accounted for 51 % of the theoretically predicted methane production value according to reaction [3]. Archaeal clones based on the 16S rRNA gene sequences were analyzed, and methanogens within the order of *Methanomicrobiales* and *Methanosarcinales* were prevalent

**Table 3** Chemical processes involved in the anaerobic degradation of palmitate

| | | | |
|---|---|---|---|
| Route 1 Bioconversion of palmitate to $H_2$ and $CO_2$, linked to methanogenesis from $CO_2$ reduction | | | |
| | $C_{16}H_{31}O_2^- + 30H_2O + H^+ = 16CO_2 + 46H_2$ | $\Delta G^{o\prime}$ = 1105 kJ/mol | [1] |
| | $46H_2 + 11.5CO_2 = 11.5CH_4 + 23H_2O$ | $\Delta G^{o\prime}$ = -1503.6 kJ/mol | [7] |
| SUM | $C_{16}H_{31}O_2^- + 7H_2O + H^+ = 11.5CH_4 + 4.5CO_2$ | $\Delta G^{o\prime}$ = -398.6 kJ/mol | [5] |
| Route 2 Bioconversion of palmitate to acetate and $H_2$, linked to acetoclastic methanogenesis and $CO_2$ reduction | | | |
| | $C_{16}H_{31}O_2^- + 14H_2O = 8CH_3COO^- + 14H_2 + 7H^+$ | $\Delta G^{o\prime}$ = 344.9 kJ/mol | [8] |
| | $8CH_3COO^- + 8H^+ = 8CH_4 + 8CO_2$ | $\Delta G^{o\prime}$ = -285.9 kJ/mol | [9] |
| | $14H_2 + 3.5CO_2 = 3.5CH_4 + 7H_2O$ | $\Delta G^{o\prime}$ = -457.6 kJ/mol | [10] |
| SUM | $C_{16}H_{31}O_2^- + 7H_2O + H^+ = 11.5CH_4 + 4.5CO_2$ | $\Delta G^{o\prime}$ = -398.6 kJ/mol | [5] |
| Route 3 Bioconversion of palmitate to acetate and $H_2$, linked to syntrophic acetate oxidation and methanogenesis from $CO_2$ reduction | | | |
| | $C_{16}H_{31}O_2^- + 14H_2O = 8CH_3COO^- + 14H_2 + 7H^+$ | $\Delta G^{o\prime}$ = 344.9 kJ/mol | [8] |
| | $8CH_3COO^- + 8H^+ + 16H_2O = 32H_2 + 16CO_2$ | $\Delta G^{o\prime}$ = 760.1 kJ/mol | [11] |
| | $46H_2 + 11.5CO_2 = 11.5CH_4 + 23H_2O$ | $\Delta G^{o\prime}$ = -1503.6 kJ/mol | [7] |
| SUM | $C_{16}H_{31}O_2^- + 7H_2O + H^+ = 11.5CH_4 + 4.5CO_2$ | $\Delta G^{o\prime}$ = -398.6 kJ/mol | [5] |
| Route 4 Bioconversion of palmitate to acetate and $H_2S$ under the condition of sulfate addition, linked to acetoclastic methanogenesis | | | |
| | $C_{16}H_{31}O_2^- + 3.5SO_4^{2-} = 8CH_3COO^- + 3.5H_2S$ | $\Delta G^{o\prime}$ = -207.2 kJ/mol | [12] |
| | $8CH_3COO^- + 8H^+ = 8CH_4 + 8CO_2$ | $\Delta G^{o\prime}$ = -285.9 kJ/mol | [9] |
| SUM | $C_{16}H_{31}O_2^- + 3.5SO_4^{2-} + 8H^+ = 8CH_4 + 8CO_2 + 3.5H_2S$ | $\Delta G^{o\prime}$ = -493.1 kJ/mol | [6] |
| Route 5 Bioconversion of palmitate to acetate and $H_2S$ under the condition of sulfate addition, linked to syntrophic acetate oxidation and methanogenesis from $CO_2$ reduction | | | |
| | $C_{16}H_{31}O_2^- + 3.5SO_4^{2-} = 8CH_3COO^- + 3.5H_2S$ | $\Delta G^{o\prime}$ = -207.2 kJ/mol | [12] |
| | $8CH_3COO^- + 8H^+ + 16H_2O = 32H_2 + 16CO_2$ | $\Delta G^{o\prime}$ = 760.1 kJ/mol | [11] |
| | $32H_2 + 8CO_2 = 8CH_4 + 16H_2O$ | $\Delta G^{o\prime}$ = -1046 kJ/mol | [13] |
| SUM | $C_{16}H_{31}O_2^- + 3.5SO_4^{2-} + 8H^+ = 8CH_4 + 8CO_2 + 3.5H_2S$ | $\Delta G^{o\prime}$ = -493.1 kJ/mol | [6] |

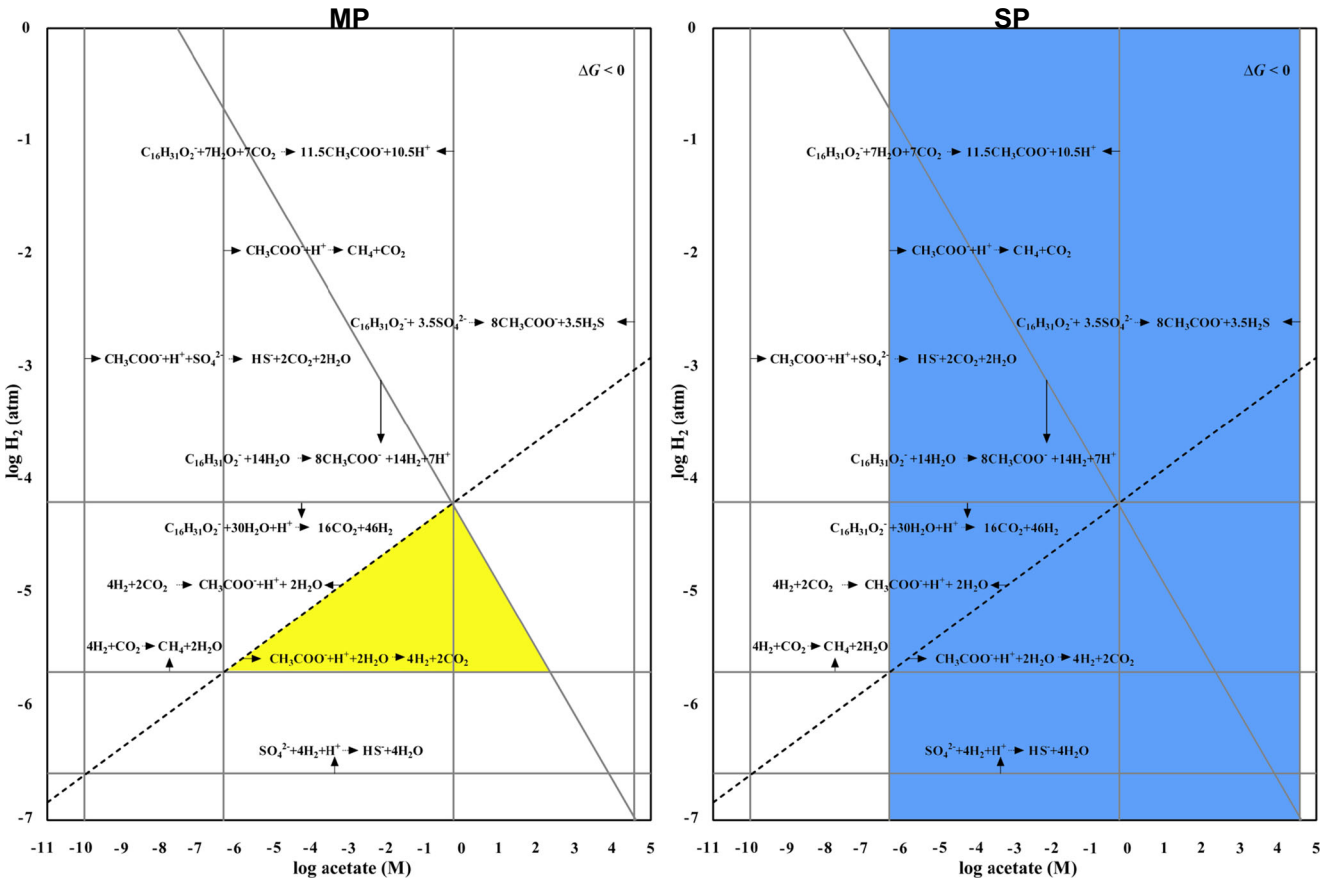


**Fig. 5** Hydrogen and acetate as thermodynamic constrains on methanogenic palmitate degradation in sample MP and SP. The window of opportunity for the methanogenic pathways in sample MP is indicated in *yellow color*; incomplete oxidation of palmitate to acetate and hydrogen was linked to syntrophic acetate oxidation and methanogenesis from $CO_2$ reduction. The window of opportunity for the methanogenic pathways in sample SP is indicated in *blue color*; incomplete oxidation of palmitate to acetate and hydrogen sulfide was linked to acetoclastic methanogenesis

in the enrichment cultures. Genus *Methanocalculus* (representing 83.8 % of all archaeal sequences in MP-A), which could utilize $H_2/CO_2$ and formate as substrates of methanogenesis (Lai et al. 2002; Grabowski et al. 2005), plays the dominant role in the methane-producing process, thus implies that palmitate degradation to methane is a $CO_2$-reducer process. The presence of *Methanosarcina* (representing 5.4 % of all archaeal sequences in MP-A) and *Methanosaeta* (representing 10.8 % of all archaeal sequences in MP-A) also dictates other methanogenic pathways. qPCR analysis shows that major archaeal belongs to *Methanomicrobiales* also support this conjecture. Unclassified Bacteria and *Thermotogae* dominated the clone library constructed from the palmitate-based enrichment, implying that members of these bacteria would have contributed to the degradation of palmitate. $H_2$ was not detectable during the incubation period of this study; therefore, we postulate that hydrogen was immediately consumed after it was produced. At the same time, metabolites such as formate, acetate, and propionate were formed in the enrichment culture. In comparison to the control incubation (M0, Table 1), there was a net positive accumulation of formate and acetate in MP samples with formate concentration four times higher than M0. This observation indicates that formate might also be an important precursor of methane production in MP. Acetate would have been produced from palmitate according to equation [8]. Formate could have been produced through syntrophic acetate oxidation (Dolfing 2014). In this enrichment, net methane production reached 1323 μmol/microcosm; formate and acetate production was 192.5 and 110.6 μmol/microcosm, respectively. From these values, we can estimate from equation [5] that when 1323 μmol/microcosm of methane was produced, 517.7 μmol/microcosm of $CO_2$ would be generated, higher than the amount detected 200 μmol/microcosm, indicating that syntrophic acetate oxidation might take place in this sample.

## Methane formation in the presence of sulfate

According to the $\Delta G^{\circ}$ values of reaction [6], degradation of palmitate to methane with the addition of sulfate is a feasible process. However, it has been reported that little or no methane would be produced with sulfate as exogenous electron

acceptors and palmitate as the sole carbon source (Colleran et al. 1995; Sousa et al. 2009). It is obvious that sulfate addition had significant impact on the microbial community structure in SP enrichment in comparison to MP. But, methane production could reach 1064 μmol/microcosm in SP, 75.6 % of the methane formed in MP (or 80.3 % of the net methane produced in MP with respect to the control incubation), which was not as small as reported previously (Sousa et al. 2009). This observation indicated that the presence of sulfate and/or sulphidogenesis had some impact on the total methane production in SP compared with MP, but methanogenesis was not inhibited even though 96.2 % of the sulfate amended was consumed. Majority of the archaeal sequences were affiliated with the genus *Methanosaeta* (representing 93.2 % of all archaeal sequences in SP-A), a typical acetoclastic methanogen (Smith and Ingram-Smith 2007; Qu et al. 2009). These archaeal members would have contributed to the acetoclastic production of methane in SP, and it seems that the presence of sulfate did not hinder the enrichment of these methanogens. Or other methanogens such as *Methanocalculus* and *Methaosarcina*, detected in sample MP, were inhibited by the presence of sulfate or by the activities of sulphidogenic microorganisms. The enrichment of *Desulfococcus*, *Desulfarculus*, and unclassified *Desulfobulbaceae* was a result of sulfate reduction because members of these groups could complete/incomplete degrade short/long-chain fatty acids (Sousa et al. 2010; Kuever 2014c; b, a). Besides the sulfate-reducing bacteria, *Smithella* plays a key role in hydrocarbon contained systems, is responsible for alkane activation and LCFAs oxidation (Gray et al. 2011; Embree et al. 2014; Tan et al. 2014), and was also detected in SP. This observation agrees with the fact that more palmitate was consumed and more acetate was produced in SP than in MP.

### Effects of sulfate on methanogenesis

Sulfate addition promoted the enrichment of *Desulfococcus*, *Desulfarculus*, and unclassified *Desulfobulbaceae*, microorganisms that were not detected in MP and S0. The methane produced in both settings based on the above described reactions, approximately 240.3 μmol and 287.1 μmol of palmitate were available for methane formation in MP and SP, respectively. Quantitatively, methane production in sulfate amended cultures was almost 1/4 less than that produced in MP indicating that the presence of sulfate promoted the growth and enrichment of microbes competing for substrates with methanogens. Alternatively, the 1/4 less methane produced in SP also agrees with the different postulated bioconversion routes of palmitate in MP and SP. Indeed, according to the stoichiometry in reactions [5] and [6], methane produced in sample SP was always about 1/3 lower than that produced in sample MP. According to our detection, 50.9 and 71 % of substrate carbon were recovered in MP and SP, respectively. Since no other LCFAs were detected in the liquid phase of both samples, dissolved $CO_2$ was not detected; the actual carbon recovery values of both MP and SP should be higher than the above calculations. These values are acceptable with respect to the long-term incubation period used in this study.

### Thermodynamic constraints on sulfate-dependent methanogenic conversion of palmitate

The thermodynamic calculations presented here indicated that methanogenic palmitate degradation is an exergonic process. The Gibbs free energy calculations also indicate that conversion of palmitate to acetate in the presence of sulfate as electron acceptor is exergonic even at high acetate concentrations (Fig. 5, SP). Comparing MP with SP (Fig. 5), the window of opportunity for linking conversion of palmitate to acetate with acetoclastic methanogenesis in the presence of sulfate is much higher than other equivalent windows for linking incomplete oxidation of palmitate to both acetoclastic methanogenesis and methanogenic $CO_2$ reduction. This suggests that acetoclastic methanogenesis plays a dominant role in palmitate-degrading systems in the presence of sulfate. Furthermore, this experimental determination of methanogenic pathways with oil field production water also suggest that acetoclastic methanogenesis may be more important than $CO_2$ reduction to methane in petroleum reservoir production water in the presence of sulfate.

Oil reservoirs can be considered as enormous anaerobic bioreactors that contain thousands of distinctively different chemical compounds (e.g., hydrocarbons, long/short chain fatty acids, and other organic/inorganic compounds) (Jones et al. 2000; Meredith et al. 2000; Mbadinga et al. 2011). Anaerobic degradation of these coumpounds to methane involves the participation of a variety of microorganisms. It has been reported that the addition of electron acceptors could alter/accelerate methanogenic pathways. The increase in $CO_2$ pressure accelerates the rate of methanogenesis to more than twice than that under low $CO_2$ conditions (Mayumi et al. 2013). Sulfate, a typical electron acceptor, is commonly detected in oil resevoir environments. The presence of sulfate could influence methanogenic process since many sulfate reducing bacteria have the ability to utilize alkanes/LCFAs to form methanogenic precursors (e.g., acetate) which could then be converted to methane by methnaogens. According to Callbeck et al. (2013), conversion of hexadecane with sulfate to acetate is feasible, providing new information on the mechanism of oil degradation under sulfate-reducing conditions. Our research indicates that methanogenesis from palmitate in the presence of sulfate was highly active in low temperature production water of oilfield. The conversion of palmitate to acetate with sulfate as an electron acceptor (Fig. 5) is thermodynamically feasible. There were considerable differences between the two microbial communities under

the treatments. *Methanosaeta* were typical acetoclastic methanogens enriched in the enrichment cultures amended with palmitate and sulfate, whereas *Methanocalculus* were predominantly enriched in enrichment cultures with palmitate only. These observations suggest that the main biochemical pathway of palmitate conversion in the microcosms amended with palmitate alone was via syntrophic acetate oxidation (SAO) coupled with $CO_2$-reduction or alternatively methane could be formed through utilization of formate, whereas addition of sulfate and/or the activity of sulfate reducers changed the methanogenic pathways to acetoclastic ones.

In summary, palmitate could be converted to methane either with or without sulfate. Without sulfate, $CO_2$-reducing methanogenesis was the dominant biochemical pathway, but, in the presence of sulfate acetoclastic methanogenesis was promoted. These results suggested that acetoclastic methanogenesis was not inhibited or affected largely by the presence of sulfate, allowing a better understanding on the presence of sulfate to the methanogenic biochemical process.

**Acknowledgments** This work was supported by the National Natural Science Foundation of China (Grant No. 51174092, 41373070, 31200101), the National Natural Science Foundation of China, and the Research Grants Council Joint Research Fund (Grant No. 41161160560).

**Conflict of interest** The authors declare no competing financial interests.

## References

Altschul SF, Gish W, Miller W, Myers EW, Lipman DJ (1990) Basic local alignment search tool. J Mol Biol 215:403–410. doi:10.1016/S0022-2836(05)80360-2

Amend JP, Shock EL (2001) Energetics of overall metabolic reactions of thermophilic and hyperthermophilic Archaea and Bacteria. FEMS Microbiol Rev 25:175–243. doi:10.1111/j.1574-6976.2001.tb00576.x

Ashelford KE, Chuzhanova NA, Fry JC, Jones AJ, Weightman AJ (2006) New screening software shows that most recent large 16S rRNA gene clone libraries contain chimeras. Appl Environ Microbiol 72:5734–5741. doi:10.1128/AEM.00556-06

Beckmann S, Lueders T, Krüger M, Von Netzer F, Engelen B, Cypionka H (2011) Acetogens and acetoclastic *Methanosarcinales* govern methane formation in abandoned coal mines. Appl Environ Microbiol 77:3749–3756. doi:10.1128/aem.02818-10

Callaghan AV, Gieg LM, Kropp KG, Suflita JM, Young LY (2006) Comparison of mechanisms of alkane metabolism under sulfate-reducing conditions among two bacterial isolates and a bacterial consortium. Appl Environ Microbiol 72:4274–4282. doi:10.1128/aem.02896-05

Callbeck CM, Agrawal A, Voordouw G (2013) Acetate production from oil under sulfate-reducing conditions in bioreactors injected with sulfate and nitrate. Appl Environ Microbiol 79:5059–5068. doi:10.1128/aem.01251-13

Cheng L, Qiu TL, Yin XB, Wu XL, Hu GQ, Deng Y, Zhang H (2007) *Methermicoccus shengliensis* gen. nov., sp. nov., a thermophilic, methylotrophic methanogen isolated from oil-production water, and proposal of *Methermicoccaceae* fam. nov. Int J Syst Evol Microbiol 57:2964–2969. doi:10.1099/ijs.0.65049-0

Cheng L, Shi S, Li Q, Chen J, Zhang H, Lu Y (2014) Progressive degradation of crude oil *n*-alkanes coupled to methane production under mesophilic and thermophilic conditions. PLoS ONE 9, e113253. doi:10.1371/journal.pone.0113253

Colleran E, Finnegan S, Lens P (1995) Anaerobic treatment of sulphate-containing waste streams. Antonie Leeuwenhoek 67:29–46. doi:10.1007/bf00872194

Cravo-Laureau C, Grossi V, Raphel D, Matheron R, Hirschler-Réa A (2005) Anaerobic *n*-alkane metabolism by a sulfate-reducing bacterium, *Desulfatibacillum aliphaticivorans* Strain CV2803T. Appl Environ Microbiol 71:3458–3467. doi:10.1128/aem.71.7.3458-3467.2005

Dolfing J (2014) Thermodynamic constraints on syntrophic acetate oxidation. Appl Environ Microbiol 80:1539–1541. doi:10.1128/aem.03312-13

Dolfing J, Larter SR, Head IM (2008) Thermodynamic constraints on methanogenic crude oil biodegradation. ISME J 2:442–452. doi:10.1038/ismej.2007.111

Dolfing J, Xu A, Gray ND, Larter SR, Head IM (2009) The thermodynamic landscape of methanogenic PAH degradation. Microb Biotechnol 2:566–574. doi:10.1111/j.1751-7915.2009.00096.x

Embree M, Nagarajan H, Movahedi N, Chitsaz H, Zengler K (2014) Single-cell genome and metatranscriptome sequencing reveal metabolic interactions of an alkane-degrading methanogenic community. ISME J 8:757–767. doi:10.1038/ismej.2013.187

Fu L, Niu B, Zhu Z, Wu S, Li W (2012) CD-HIT: accelerated for clustering the next-generation sequencing data. Bioinformatics 28:3150–3152. doi:10.1093/bioinformatics/bts565

Grabowski A, Blanchet D, Jeanthon C (2005) Characterization of long-chain fatty-acid-degrading syntrophic associations from a biodegraded oil reservoir. Res Microbiol 156:814–821. doi:10.1016/j.resmic.2005.03.009

Gray ND, Sherry A, Grant RJ, Rowan AK, Hubert CRJ, Callbeck CM, Aitken CM, Jones DM, Adams JJ, Larter SR, Head IM (2011) The quantitative significance of *Syntrophaceae* and syntrophic partnerships in methanogenic degradation of crude oil alkanes. Environ Microbiol 13:2957–2975. doi:10.1111/j.1462-2920.2011.02570.x

Guan J, Xia LP, Wang LY, Liu JF, Gu JD, Mu BZ (2013) Diversity and distribution of sulfate-reducing bacteria in four petroleum reservoirs detected by using 16S rRNA and *dsrAB* genes. Int Biodeterior Biodegrad 76:58–66. doi:10.1016/j.ibiod.2012.06.021

Guan J, Zhang BL, Mbadinga S, Liu JF, Gu JD, Mu BZ (2014) Functional genes (*dsr*) approach reveals similar sulphidogenic prokaryotes diversity but different structure in saline waters from corroding high temperature petroleum reservoirs. Appl Environ Microbiol 98:1871–1882. doi:10.1007/s00253-013-5152-y

Huber T, Faulkner G, Hugenholtz P (2004) Bellerophon: a program to detect chimeric sequences in multiple sequence alignments. Bioinformatics 20:2317–2319. doi:10.1093/bioinformatics/bth226

Jones DM, Watson JS, Meredith W, Chen M, Bennett B (2000) Determination of naphthenic acids in crude oils using nonaqueous ion exchange solid-phase extraction. Anal Chem 73:703–707. doi:10.1021/ac000621a

Kendall M, Boone D (2006) The Order *Methanosarcinales* in Dworkin M, Falkow S, Rosenberg E, Schleifer K-H and Stackebrandt E (eds) The Prokaryotes, Springer, New York, pp 244-256. doi: 10.1007/0-387-30743-5_12

Kuever J (2014a) The Family *Desulfarculaceae*. In: Rosenberg E, DeLong EF, Lory S, Stackebrandt E, Thompson EF (eds) The Prokaryotes: *Deltaproteobacteria* and *Epsilonproteobacteria*. Springer, Berlin, pp 41–44. doi:10.1007/978-3-642-39044-9_270

Kuever J (2014b) The Family *Desulfobacteraceae*. In: Rosenberg E, DeLong EF, Lory S, Stackebrandt E, Thompson EF (eds) The

Prokaryotes. Springer, Berlin, pp 45–73. doi:10.1007/978-3-642-39044-9_266

Kuever J (2014c) The Family *Desulfobulbaceae*. In: Rosenberg E, DeLong EF, Lory S, Stackebrandt E, Thompson EF (eds) The Prokaryotes: *Deltaproteobacteria* and *Epsilonproteobacteria*. Springer, Berlin, pp 75–86. doi:10.1007/978-3-642-39044-9_267

Lai MC, Chen SC, Shu CM, Chiou MS, Wang CC, Chuang MJ, Hong TY, Liu CC, Lai LJ, Hua JJ (2002) *Methanocalculus taiwanensis* sp. nov., isolated from an estuarine environment. Int J Syst Evol Microbiol 52:1799–1806. doi:10.1099/ijs.0.01730-0

Lee ZM, Bussema C 3rd, Schmidt TM (2009) *rrn*DB: documenting the number of rRNA and tRNA genes in bacteria and archaea. Nucleic Acids Res 37(database issue):D489–D493. doi:10.1093/nar/gkn689

Li W, Godzik A (2006) Cd-hit: a fast program for clustering and comparing large sets of protein or nucleotide sequences. Bioinformatics/Comput Appl Biosci 22:1658–1659. doi:10.1093/bioinformatics/btl158

Mayumi D, Dolfing J, Sakata S, Maeda H, Miyagawa Y, Ikarashi M, Tamaki H, Takeuchi M, Nakatsu CH, Kamagata Y (2013) Carbon dioxide concentration dictates alternative methanogenic pathways in oil reservoirs. Nat Commun 4.: 1998 doi:10.1038/ncomms2998

Mbadinga SM, Wang LY, Zhou L, Liu JF, Gu JD, Mu BZ (2011) Microbial communities involved in anaerobic degradation of alkanes. Int Biodeterior Biodegrad 65:1–13. doi:10.1016/j.ibiod.2010.11.009

Mbadinga S, Li KP, Zhou L, Wang LY, Yang SZ, Liu JF, Gu JD, Mu BZ (2012) Analysis of alkane-dependent methanogenic community derived from production water of a high-temperature petroleum reservoir. Appl Environ Microbiol 96:531–542. doi:10.1007/s00253-011-3828-8

McGinnis S, Madden TL (2004) BLAST: at the core of a powerful and diverse set of sequence analysis tools. Nucleic Acids Res 32:W20–W25. doi:10.1093/nar/gkh435

Meredith W, Kelland SJ, Jones DM (2000) Influence of biodegradation on crude oil acidity and carboxylic acid composition. Org Geochem 31:1059–1073. doi:10.1016/S0146-6380(00)00136-4

Noor E, Haraldsdóttir HS, Milo R, Fleming RM (2013) Consistent estimation of Gibbs energy using component contributions. PLoS Comput Biol 9, e1003098. doi:10.1371/journal.pcbi.1003098

Pham VD, Hnatow LL, Zhang S, Fallon RD, Jackson SC, Tomb JF, Delong EF, Keeler SJ (2009) Characterizing microbial diversity in production water from an Alaskan mesothermic petroleum reservoir with two independent molecular methods. Environ Microbiol 11:176–187. doi:10.1111/j.1462-2920.2008.01751.x

Qu X, Vavilin VA, Mazéas L, Lemunier M, Duquennoi C, He PJ, Bouchez T (2009) Anaerobic biodegradation of cellulosic material: Batch experiments and modelling based on isotopic data and focusing on aceticlastic and non-aceticlastic methanogenesis. Waste Manag 29:1828–1837. doi:10.1016/j.wasman.2008.12.008

Rabus R, Hansen T, Widdel F (2013) Dissimilatory sulfate- and sulfur-reducing Prokaryotes. In: Rosenberg E, Delong E, Lory S, Stackebrandt E, Thompson F (eds) The Prokaryotes. Springer, Berlin, pp 309–404. doi:10.1007/978-3-642-30141-4_70

Savage KN, Krumholz LR, Gieg LM, Parisi VA, Suflita JM, Allen J, Philp RP, Elshahed MS (2010) Biodegradation of low-molecular-weight alkanes under mesophilic, sulfate-reducing conditions: metabolic intermediates and community patterns. FEMS Microbiol Ecol 72:485–495. doi:10.1111/j.1574-6941.2010.00866.x

Shimizu S, Upadhye R, Ishijima Y, Naganuma T (2011) *Methanosarcina horonobensis* sp. nov., a methanogenic archaeon isolated from a deep subsurface miocene formation. Int J Syst Evol Micr 61:2503–2507. doi:10.1099/ijs.0.028548-0

Smith KS, Ingram-Smith C (2007) *Methanosaeta*, the forgotten methanogen? Trends Microbiol 15:150–155. doi:10.1016/j.tim.2007.02.002

Sousa DZ, Pereira MA, Stams AJ, Alves MM, Smidt H (2007) Microbial communities involved in anaerobic degradation of unsaturated or saturated long-chain fatty acids. Appl Environ Microbiol 73:1054–1064. doi:10.1128/AEM.01723-06

Sousa DZ, Alves JI, Alves MM, Smidt H, Stams AJ (2009) Effect of sulfate on methanogenic communities that degrade unsaturated and saturated long-chain fatty acids (LCFA). Environ Microbiol 11:68–80. doi:10.1111/j.1462-2920.2008.01740.x

Sousa DZ, Balk M, Alves M, Schink B, Mcinerney MJ, Smidt H, Plugge CM, Stams AJM (2010) Degradation of long-chain fatty acids by sulfate-reducing and methanogenic communities. In: Timmis K (ed) Handbook of Hydrocarbon and Lipid Microbiology, 1st edn. Springer, Berlin, pp 963–980. doi:10.1007/978-3-540-77587-4_69

Tan B, Nesbo C, Foght J (2014) Re-analysis of omics data indicates *Smithella* may degrade alkanes by addition to fumarate under methanogenic conditions. ISME J 8:2353–2356. doi:10.1038/ismej.2014.87

Thauer RK, Jungermann K, Decker K (1977) Energy conservation in chemotrophic anaerobic bacteria. Bacteriol Rev 41(1):100–180

Wang LY, Gao CX, Mbadinga SM, Zhou L, Liu JF, Gu JD, Mu BZ (2011) Characterization of an alkane-degrading methanogenic enrichment culture from production water of an oil reservoir after 274 days of incubation. Int Biodeterior Biodegrad 65:444–450. doi:10.1016/j.ibiod.2010.12.010

Yu Y, Lee C, Kim J, Hwang S (2005) Group-specific primer and probe sets to detect methanogenic communities using quantitative real-time polymerase chain reaction. Biotechnol Bioeng 89:670–679. doi:10.1002/bit.20347

Zellner G, Messner P, Winter J, Stackebrandt E (1998) *Methanoculleus palmolei* sp. nov., an irregularly coccoid methanogen from an anaerobic digester treating wastewater of a palm oil plant in North-Sumatra, Indonesia. Int J Syst Bacteriol 48:1111–1117. doi:10.1099/00207713-48-4-1111

Zhou L, Li KP, Mbadinga S, Yang SZ, Gu JD, Mu BZ (2012) Analyses of *n*-alkanes degrading community dynamics of a high-temperature methanogenic consortium enriched from production water of a petroleum reservoir by a combination of molecular techniques. Ecotoxicology 21:1680–1691. doi:10.1007/s10646-012-0949-5

Zhu J, Zheng H, Ai G, Zhang G, Liu D, Liu X, Dong X (2012) The genome characteristics and predicted function of methyl-group oxidation pathway in the obligate aceticlastic methanogens, *Methanosaeta* spp. PLoS ONE 7, e36756. doi:10.1371/journal.pone.0036756